JOURNAL OF MATERIALS SCIENCE 33 (1998) 23–28

Effect of the cooling rate on the dendrite arm spacing and the ultimate tensile strength of cast iron

K. H. W. SEAH
Department of Mechanical Engineering, National University of Singapore, 10 Kent Ridge Crescent, Singapore 119260

J. HEMANTH
Department of Mechanical Engineering, Siddaganga Institute of Technology, Tumkur 572103, Karnataka, India

S. C. SHARMA
Department of Mechanical Engineering, R.V. College of Engineering, Mysore Road, Bangalore 560059, Karnataka, India

This paper describes a series of microstructural and strength studies performed on hypereutectic cast iron which was sand cast using a variety of end chills (metallic, non-metallic, water cooled and liquid nitrogen cooled, respectively). The effects of cooling rate on the dendrite arm spacing (DAS) and the ultimate tensile strength (UTS) were evaluated. Attempts were also made in the paper to explain these effects and to correlate the UTS with the DAS.

1. Introduction

1.1. Chilled cast iron

Chilled cast iron belongs to a group of metals possessing high strength, high hardness and high wear resistance. For a metallurgist, there is sufficient information available on the dendrite arm spacing and the solidification mode of ordinary cast iron cast in sand moulds. However, there is a dearth of information on the DAS the mode of solidification and the effect of these two on strength of chilled cast iron using various types of chill including water-cooled and liquid-nitrogen-cooled chills. This caused us to embark upon a series of experiments to find the effect of DAS and solidification on the strength of various types of chilled cast iron. The reason behind the selection of this series of chilled cast iron for the present investigation is that a wide range of ultimate tensile strength (UTS) values can be obtained with different DASs. Moreover, using such a chilling technique, a low-grade cast iron can be converted into one of superior qualities depending on the mode of solidification and the DAS.

1.2. Effect of the cooling rate during solidification

In general, the cooling rate during casting is largely governed by the design and thermal nature of the casting procedure, one significant factor being the mould material. Metal moulds generally offer a higher chilling action on the solidifying mass because of their higher heat diffusivity. The influence of the higher cooling rate is normally responsible for the superior properties of chilled castings. The use of chills firstly favours the refinement of microstructure and secondly steepens the temperature gradients, making solidification directional. The influence of very high cooling rates in producing fine structures offers the possibility of future development of cast irons possessing high strength and good wear resistance. The undercooling of a melt to a lower temperature increases the number of effective nuclei relative to the growth rate, the latter being restricted by the rate at which the latent heat of crystallization can be dissipated. On the other hand, slow cooling favours the growth from a few nuclei and produces coarse grain structures. The refining effect of an enhanced cooling rate applies both to primary grain size and to the substructure, although in the latter case the effect is on the growth process rather than on nucleation. Thus, there is a marked effect upon dendrite cell size and DAS when the cooling rates vary over a wide range.

Copper was selected as an important alloying element for hypereutetic cast iron in view of its tremendous potential as a grain refiner. Keeping in mind the above, the present research work was planned for the following purposes: (a) to obtain experimental data for the DAS with various cooling rates; (b) to analyse the data in the light of the solidification process; (c) to correlate the UTS with the DAS.

1.3. Past research

The effect of chills on the solidification characteristics of cast iron has been studied by Bishop *et al.* [1]. Berry

 © *1998 Chapman & Hall*

[2] showed the importance of the solidification time of castings. The eutectic solidification starts at certain locations and continues by radial growth with the simultaneous separation of graphite and austenite from the melt. Furthermore, the lower the temperature of formation (i.e., the greater the amount of undercooling), the finer is the graphite formed.

The decrease in the DAS spacing with increase in the cooling rate can be explained by the fact that there is insufficient time available for the diffusion of solute. Also, as the eutectic composition is approached, there is an increasing amount of solute that is rejected as the composition moves further away from the pure metal. Howarth and Mondolfo [3] concluded from their findings that the DAS was controlled by diffusion and not by heat transfer, and that the spacing was determined by the characteristic thickness of the diffusion zone around a growing dendrite. They also observed that the rate of cooling had a tremendous effect on the DAS. DASs in alloys that solidified dendritically have been investigated by Alexander and Rhines [4].

Austenite dendrite interaction was shown to be a major factor affecting the UTS of the material [5]. The influence of changes in the structure of austenite dendrite, graphite flakes and eutectic cells on the mechanical properties of the material was investigated by Ruff and Wallace [6]. They found that a high tensile strength and ductility could be obtained in as-cast grey iron by increasing the amount of graphite-free area (consisting of austenitic dendrites in most cases).

Sun and Loper [7] showed that intensive supercooling (both constitutional and thermal) in front of the chilling interface results in the development of cellular dendritic growth of the graphite into a form recognized as exploded graphite. The morphology of the exploded graphite depends on the compositional and thermal conditions present in front of the interface.

The microstructures of grey and ductile irons are determined by cooling rate, composition, nucleation and growth conditions prevailing during solidification and the transformation behaviour of austenite during cooling through the critical temperature range [8]. The dendritic structure in cast irons may be significantly refined by selected additions to the melt. The effect of this refinement is to increase the number of grains and to reduce the spacing of the secondary dendrite arms on the austenite dendrites [9].

2. Experimental procedure

2.1. Fabrication of material

Chilled cast iron alloy of the composition shown in Table I and cast using seven different types of chill were produced by casting at 1440 °C in the form of ingots. They shall henceforth be designated as specimens A, B, C, D, E, F and G as shown later in Table II. Apart from the usual alloying elements such Si, Mn, S and P, copper was also added to improve machinability as well as to act as a grain refiner.

2.2. Casting procedure

Fig. 1 shows a diagram of the mould used for producing the various ingots cast with water-cooled and

TABLE I Composition of the cast iron tested

Element	C	Si	Mn	S	P	Cu	Fe
Amount (wt%)	3.42	1.8	0.41	0.04	0.08	1.5	Balance

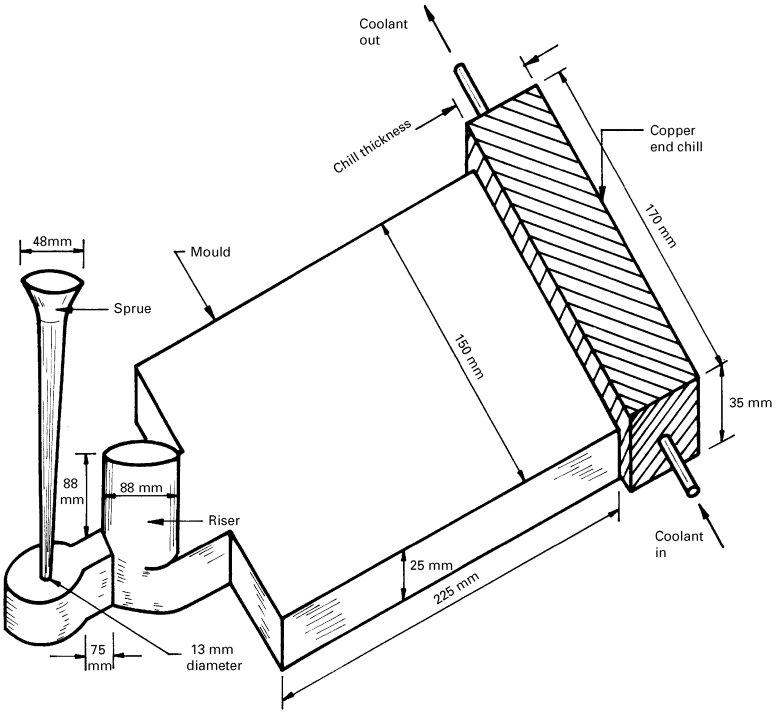

Figure 1 Mould used for casting specimens.

TABLE II UTSs (at chill end) of castings chilled using various chills

Specimen	Chill used	UTS (MPa)	Microstructure
A	Graphite	280.63	5% cementite in pearlite
B	SiC	289.44	8% cementite in pearlite
C	Cast iron	302.57	20% cementite in pearlite
D	Steel	306.46	30% cementite in pearlite
E	Copper	321.75	40% cementite in pearlite
F	Copper, water cooled	332.23	55% cementite in pearlite
G	Copper, liquid nitrogen cooled	355.89	70% cementite in pearlite

liquid-nitrogen-cooled copper chills (specimens F and G). The same type of mould was used for the other specimens too (specimens A–E) except that no liquid was passed through the chills. To make the mould for casting, a teak wood pattern of size 225 mm by 150 mm by 25 mm was employed with standard pattern allowances. The moulds were prepared using silica sand with 5% bentonite as a binder and 5% moisture. The molten alloys were cast in the mould and were cooled from one end by the chill. In the case of water-cooled chilling and liquid-nitrogen-cooled chilling, arrangements were made in the copper chill to circulate water (at 23 °C) and liquid nitrogen (at −60 °C) respectively.

2.3. Specimen selection

The specimens for microstructural and strength studies were taken from the part of the casting adjacent to the chill during casting. Tensometer specimens were prepared for strength testing (using an Instron testing machine) and the tests were performed in conformance with American Foundryman's Society standards.

Microscopic examination was conducted on all the specimens using a scanning electron microscope as well as a Neophot-21 metallurgical optical microscope. Various etchants were tried but 2% Nital proved to be the best and was therefore used.

3. Results and discussion

Table II shows the experimental results of the strength tests done on castings cast using various chills (each 25 mm thick) as well as the microstructures observed. To show the typical relationship between the DAS and the UTS along the length of the casting from the chill end to the riser end, these values for water-cooled and liquid-nitrogen-cooled chilled cast iron are listed in Tables III and IV.

3.1. Microstructural examination

Primary austenite dendrite was observed in all the specimens tested (Figs 2–8), with variations in pattern occurring as a result of differences in the rate of cooling. For each specimen, the structure of the dendrites was analysed by determining the secondary DAS, the average dendrite length, the dendrite interaction and the directionality. Marked changes were also seen in the graphite morphology as the rate of cooling was varied using different types of chill.

TABLE III DASs and UTSs of water-cooled chill cast iron along length of casting

Specimen location (distance from chill end) (mm)	DAS (μm)	UTS MPa
0.0 (at chill end)	2	332.23
30.0	3	318.57
70.0	5	306.12
105.0	5	248.78
145.0	7	243.12
180.0	10	253.25
225.0 (at riser end)	10	252.76

TABLE IV DASs and UTSs of liquid-nitrogen-cooled chill cast iron along the length of casting

Specimen location (distance from chill end) (mm)	DAS (μm)	UTS MPa
0.0 (at chill end)	1	355.89
30.0	1	312.54
70.0	4	295.43
105.0	6	244.53
145.0	8	248.21
180.0	9	259.12
225.0 (at riser end)	9	257.65

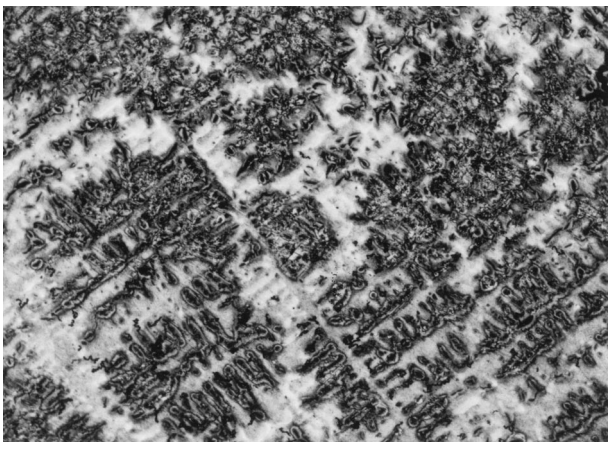

Figure 2 Photomicrograph of specimen A (cast with graphite end chill). (Magnification, 1000 × .)

Primary austenite dendrites would be expected to develop within each of the castings produced in such a manner that their solidification is dependent on the rate of undercooling. For the cast iron of hypereutectic composition selected for the present investigation,

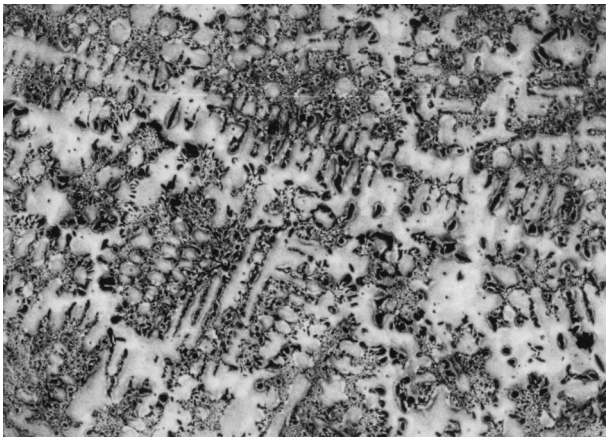

Figure 3 Photomicrograph of specimen B (cast with SiC end chill). (Magnification, 1000 × .)

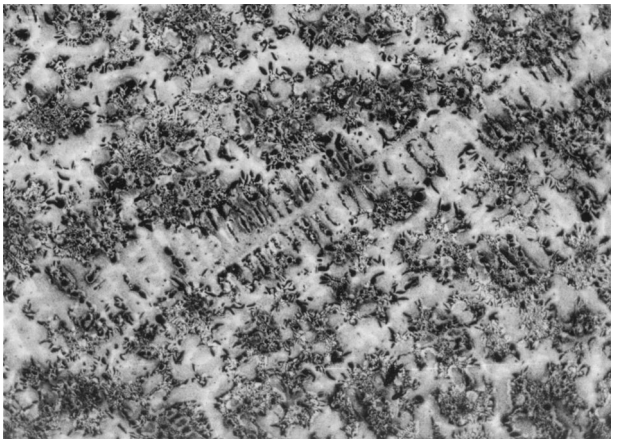

Figure 4 Photomicrograph of specimen C (cast with cast iron end chill). (Magnification, 1000 × .)

Figure 5 Photomicrograph of specimen D (cast with steel end chill). (Magnification, 1000 × .)

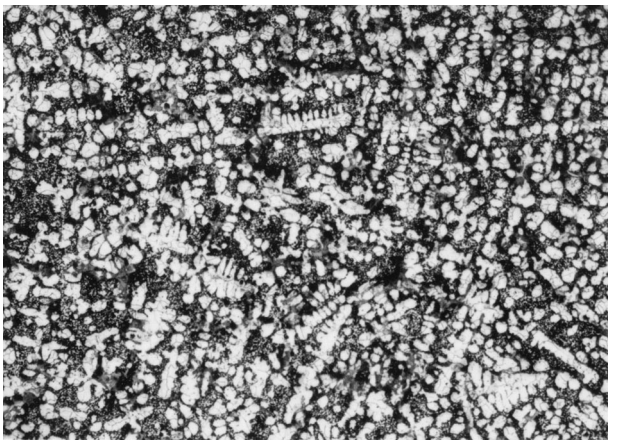

Figure 6 Photomicrograph of specimen E (cast with copper end chill). (Magnification, 1000 × .)

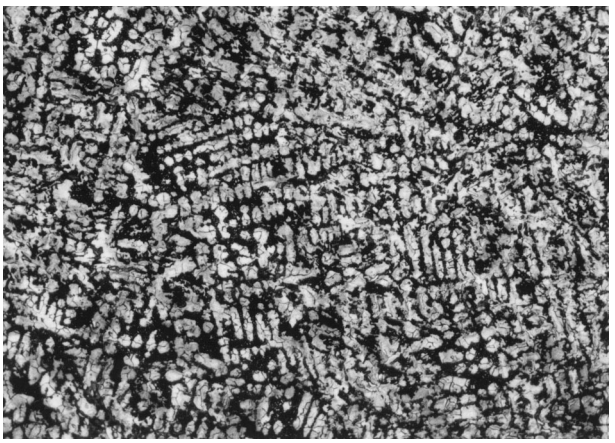

Figure 7 Photomicrograph of specimen F (cast with water-cooled end chill). (Magnification, 1000 × .)

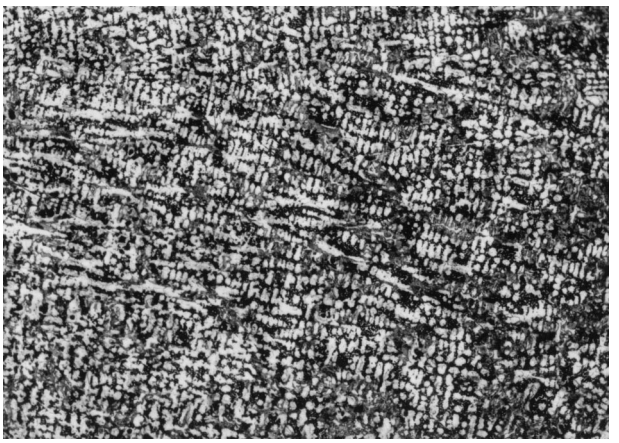

Figure 8 Photomicrograph of specimen G (cast with liquid-nitrogen-cooled copper end chill). (Magnification, 1000 × .)

because of the cooling provided during solidification, it is believed that the dendrites form prior to nucleation and growth of the eutectic. The eutectic then completes solidification by filling in the areas surrounding the dendrites. The resulting structures of transformed primary austenite dendrites traverse a number of eutectic cells, which contain both graphite and transformed eutectic austenite. According to some investigations [10], primary austenite dendrites form in hypereutectic grey irons only in the localized areas of carbon depletion near the primary graphite phase, which presumably solidifies first. However, in the present investigation, the observed formation of primary dendrites in the hypereutectic iron prior to the solidification of graphite can be explained by the relatively fast cooling and the undercooling needed for graphite nucleation. This is consistent with the arguments put forward by Ruff and Wallace [6].

In addition, dendrite interaction, which is a visual estimate of the percentage area of dendrites interesecting in a field of view, varied in the specimens tested. The largest degree of dendrite interaction was observed in cast irons chilled using high cooling rates. Figs 2–8 are photomicrographs showing the microstructures (at the chill end) of specimens A–G respectively. These are arranged in order of cooling rate, starting from Fig. 2 (specimen A) in which the rate of cooling is lowest to Fig. 8 (specimen G) in which the rate of cooling is highest. Figs 2–8 also show a variety of dendrites, ranging from large oriented dendrites to very small dendrites depending on the cooling rate during solidification. In Fig. 2, a relatively low dendrite interaction is seen. This gradually increases all the way to Fig. 8 which shows a relatively high dendrite interaction. Studies by other researchers on the difference in dendrite length, randomness and associated graphite and matrix structures show that quick cooling produces fine dendrites [11]. Other factors such as inoculation, alloy content, prior melt history and carbon equivalent may also affect the dendrite morphology but, in the present investigation, the main factor affecting dendrite morphology seems to be the cooling rate during solidification.

Solidification over a temperature range is the primary requirement for dendrite growth. Primary austenite dendrites readily grow, starting from the liquidus down to the eutectic temperature. Growth of dendrites may also continue concurrently with the eutectic as the temperature decreases through the eutectic range of the solidus. Thus, undercooling may lead to higher dendrite interaction, which is true in the case of cast iron chilled using liquid nitrogen, as confirmed by some previous research by the present authors [12]. It was also reported in that paper [12] that close to the chill, where the rate of heat extraction is greatest, a fine dendrite structure is obtained whereas, as distance from the chill increases, the spacing of the dendrites becomes larger and the number of dendrites decreases.

3.2. Dendritic arm spacing

Close observation of the photomicrographs show the existence of cored dendrites (dark areas) and interdendritic eutectic (light areas). Fig. 9 is a plot showing the relationship between the DAS and the distance from the chill end for the water-cooled and the liquid-nitrogen-cooled specimens, respectively (specimens F and G). These two modes of cooling are selected for the graphs because they are the fastest and hence give the most spectacular results. Figs 10 and 11 show the microstructures of the cast iron specimens (at the chill end) chilled using water-cooled and liquid-nitrogen-cooled chills, respectively (specimens F and G), in which a high concentration of cementite can be seen in the pearlite matrix. It can be seen from Fig. 9 that the DAS increases monotonically as the distance from the chill end increases (i.e., as the rate of cooling decreases). The DAS increases as the cooling rate decreases because there is less time available for diffusion of the solute. Hence, it is believed that diffusion controls the secondary DAS, a deduction confirmed by the work of other researchers [13].

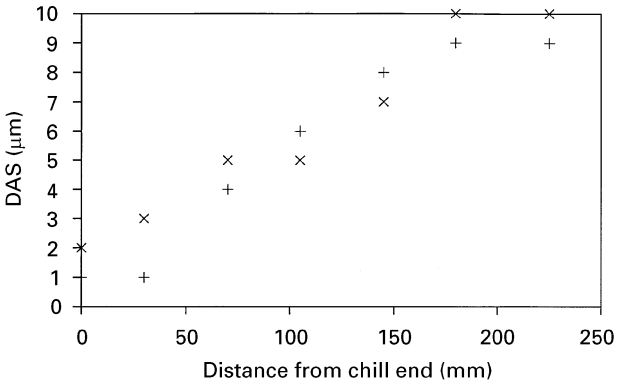

Figure 9 Relationship between DAS and distance from chill end for the water-cooled specimen F (×) and the liquid-nitrogen-cooled specimen G (+).

Figure 10 Microstructure of water-cooled chilled cast iron. (Magnification, 500×.)

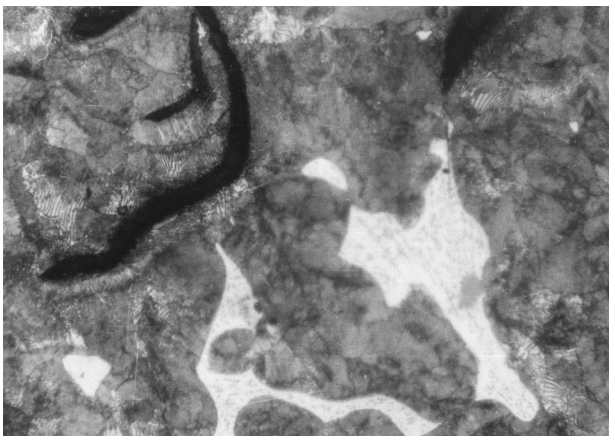

Figure 11 Microstructure of liquid-nitrogen-cooled chilled cast iron. (Magnification, 500×.)

3.3. Ultimate tensile strength

Table II shows the UTS of the cast iron specimens (at the chill end) chilled using various types of chills. Fig. 12 is a plot showing the relationship between the UTS and the DAS for the water-cooled specimen (F) and the liquid-nitrogen-cooled specimens. It can be seen that the UTS decreases monotonically as the

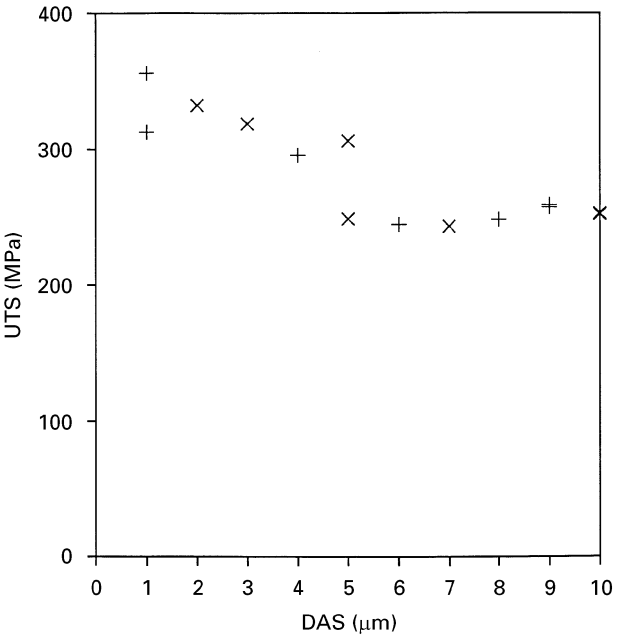

Figure 12 Relationship between UTS and DAS for the water-cooled specimen F (×) and the liquid-nitrogen-cooled specimen G (+).

DAS increases, i.e., moving away from the chill end towards the riser end. Tensile tests reveal that the larger dendrite interaction of undercooled irons explain why higher strengths are associated with them. Higher dendritic interaction areas reflect the interweaving of dendrites through eutectic cells that effectively tie the eutectic cells together. Since dendrites are formed from primary austenite and do not contain flake carbon, they have higher fracture stress than eutectic liquid that decomposed to form austenite and eutectic carbon. As the DAS increases beyond 5 μm, however, the UTS does not seem to vary much. This indicates that, for DASs above 5 μm, the rate of cooling is so slow that there is no supercooling effect and the UTS approaches that of the fully annealed cast iron.

4. Conclusions

Analysis of data on cast irons chilled using various types of chill has shown that the cooling rate has a marked effect on the DAS. The DAS was found to vary inversely with the rate of cooling. The UTS however, increases as rate of cooling increases, showing an inverse relationship with the DAS. If the rate of cooling is reduced beyond a certain point, the UTS approaches an asymptotic value, which is the UTS of fully annealed cast iron.

References

1. H. K. BISHOP, F. A. BRANT and W. S. PELLINI, *Trans. Amer. Foundryman's Soc.* **59** (1951) 435.
2. J. T. BERRY, *ibid.* **78** (1970) 421.
3. J. A. HOWARTH and L. F. MONDOLFO, *Acta Metall.* **10** (1962) 1037 (quoted by K. S. Pandey and P. Kumar, *Indian Foundry J.* (1979) 4).
4. B. H. ALEXANDER and M. B. RHINES, *Trans. AIME* **188** (1950) 1267 (quoted by K. S. Pandey and P. Kumar, *Indian Foundry J.* (1979) 4).
5. D. GLOVER and C. E. BATES, *Trans. Amer. Foundryman's Soc.* **90** (1982) 745.
6. G. F. RUFF and J. F. WALLACE, *ibid.* **85** (1977) 179.
7. G. X. SUN and C. R. LOPER, *ibid.* **91** (1983) 841.
8. J. F. WALLACE, *ibid.* **88** (1975) 363.
9. N. CHURCH, P. F. WIESER and J. F. WALLACE, *ibid.* **74** (1966) 113.
10. G. F. RUFF and J. F. WALLACE, *ibid.* **84** (1976) 705.
11. J. HEMANTH, PhD thesis, University of Mysore, Mysore (July 1995).
12. K. H. W. SEAH, J. HEMANTH and S. C. SHARMA, *Wear* **192** (1996) 134.
13. A. B. MICHAEL and M. B. BEVER, *Trans. AIME* **188** (1950) 47.

Received 9 June
and accepted 30 July 1997